# 4-DoF Spherical Parallel Wrist with Embedded Grasping Capability for Minimally Invasive Surgery

Wissem Haouas, Redwan Dahmouche, Nadine Le Fort-Piat, Guillaume J. Laurent

***Abstract*— This paper presents preliminary results of a new robotic wrist for minimally invasive surgery. This wrist is a high-dexterity miniature robot, able to provide simultaneously the grasping/cutting (1-DoF) and rotations capabilities with 3-DoF. The grasping function is insured by the folding of the top platform of a parallel structure. The grasping capability of the wrist is part of the mechanical structure itself and can be fully controlled by external actuators. In order to validate this original approach, an experimental prototype has been fabricated using 3D printing technology at a larger scale. The inverse kinematic model has been developed and the workspace analysis was accomplished to assess the capabilities of the realized system. Finally, experimental tests have been also carried out for validating the proposed structure.**

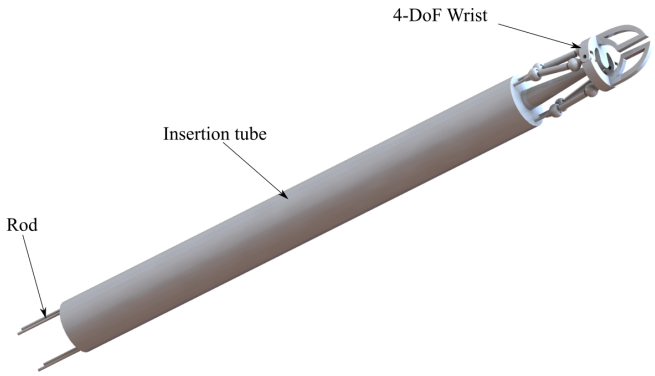


Fig. 1. Overview of the complete wrist at the tip of an instrument

## I. Introduction

In the last decades, miniaturized robots have attracted a lot of attention from academic and industrial communities from a wide fields of applications. In medical field, miniaturized systems can find their application with the light-load requirements from manipulating medical devices to precision surgery. In minimally invasive surgery, surgeons use a variety of techniques to operate with less injury to the body than with open surgery, through small openings or natural ways. In this procedure, 5-10 mm diameter instruments (graspers, scissors, clip applier) can be introduced by the surgeon into the body through trocars. The incisions should be made as much as necessary but as small as possible, as it is closely related to procedural complication and recovery.

The restricted vision, the difficulty in handling instruments (new hand-eye coordination skills are needed), the lack of tactile perception and the limited working area are factors which add to the technical complexity of this surgical approach. Thereby, robotic surgery has come up as a reference aimed at overcoming the main limitations of minimally invasive procedures, providing more dexterity to the surgeon and more accurate motion of the tools.

A relatively large number of articles are published each year on topics related to micromechanisms used in medicine for diagnostic and surgery [1] [2] [3] [4] [5] [6]. Indeed, many constraints have to be overcome in order to design a micromechanism, like the limited space and biocompatibility. Many robotic systems designed to operate as a surgical system have been presented in literature, such as ViaCath robotic system [7] and [8]. Kaouk et al. reported a single-port robotic laparoscopy procedures on humans using the daVinci system [9], which is mainly used for standard laparoscopic procedures. In 2010 the TransEntreix medical device company has introduced the SPIDER (Single Port Instrument Delivery Extended Reach) surgical system [10] and in 2012 Niccolini presented the SPRINT robot [11], these robots are designed for Single Incision Laparoscopic Surgery.

The objective of this work is to develop a new approach of robotic wrist mounted at the tip of an instrument Fig. 1. The new robotic wrist, can undertake the tasks of gripping or cutting the target tissues. In order to handle various tasks during the surgery, this robotic structure has 4-DoF. Yet, the main innovation in our system is the use of a novel parallel robotic structure based on a foldable platform.

In order to reach and examine various critical regions, the control of motion of the end effectors of surgical instruments is provided through rods system. Hence, parallel manipulators are able to provide many DoFs using linear actuators. In addition to integrate the gripping capability, we propose the addition of a degree of freedom to reconfigure the shape of the platform and use it as a grasping tool. Thus, the use of a foldable platform instead of a rigid platform allows the robot to control a two fingers of a gripper or a scissors. Some of the links of this configurable end-effector are attached to the legs so its configuration can be fully controlled from the actuators located outside the body. The originality of this architecture is that it can perform the grasping and a 3-DoF rotations simultaneously in a very compact design.

The authors are with FEMTO-ST Institute, AS2M department, Univ. Bourgogne Franche-Comté, UFC-ENSMM, Besançon, France.

Compared to serial kinematic structures found in most robotic structure designed for minimally invasive surgery parallel manipulators have the desirable characteristics of high payload and rigidity. Moreover, regarding the allowed dimensions for MIS, the joints can be replaced by flexible articulations.

The paper specifically focuses on the validation of the new robotic architecture before integrating it at the tip of an instrument.

In the next section, we present the kinematic of the new wrist and some related works. Then, we determine the inverse kinematic model. Finally, we present the design of the robot, the workspace analysis and some experimental results that describe a proof of concept constructed at a larger scale with a 3D printing machine.

## II. Kinematic structure

This section introduces the novel wrist and its kinematic structure. This new type of architecture replaces the rigid platform of a regular parallel robot by a foldable end-effector in order to provide the grasping capabilities. The proposed wrist is similar to parallel structure with a regid platform, with 3-DoF in rotations using 4 spherical joints, used in Vertical Motion Simulator [12]. Similarly, in medical field, Merlet [13] presented a micro parallel robot MIPS having 3-DoF that allows fine positioning of a surgical tool.

A relatively few articles are published on topic relates to parallel robots with configurable platform. Some of this architectures use the configurable platforms to provide rotation via a gearing system like the Par4 [14], while others use it for grasping. In 2002, Yi and al. [15] proposed a planar parallel mechanism with a parallelogramic planar platform that can be used as a gripper. Then, Mohamed and Gosselin [16] proposed in 2005, a first generalization of the concept of both planar and spatial parallels robots with configurable platforms. Lambert [17] presented a 5-DoF parallel manipulator that generates 3 translations, 1 rotation plus a linear grasping motion. Also, in 2015 Lambert [18] introduced a novel redundantly activated parallel architecture that provides 6-DoF motion and 1-DoF grasping capabilities.

The main innovation in our structure is the presence of a 1-DoF foldable platform instead of a closed loop chain found in most parallel robots with configurable platform. This additional DoF is more compact and provides grasping capability via two fingers located on the platform.

The concept of our structure is described by the architectural scheme illustrated in Fig. 2, where joints are represented by rectangles and links between those joints are represented by lines.

The robot is composed of three main parts: four linear actuators, five struts and a foldable platform where the two finger gripper are fixed. The platform is formed by two semicircles assembled by a revolute joint. Two fingers are attached to each part of the platform can be used as a gripper, scissors, etc... Each part of the platform has two struts attached to points $A_i$, where universal joints connect the 4 parallel struts to the configurable platform. Every strut is attached to a prismatic linear axis via a spherical joint. The configuration of the platform is defined by the angular folding value $\theta$. The position of the platform is defined by the 3 Bryan angles $(\alpha, \beta, \gamma)$ to describe the relative orientation of the platform with the base. In order to eliminate any displacement of the platform, a central strut fixed on the base and connected to one part of the deformable platform through a spherical joint is used.

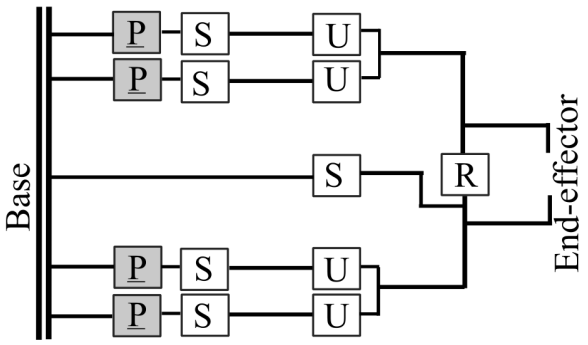


Fig. 2. Architectural scheme of the manipulator. Let P, R, U and S represent prismatic, revolute, universal and spherical joint, respectively.

The orientation and the grasping configuration of the platform are controlled by 4 vertical parallel linear actuators located away from the structure. Each struts have a prismatic 1-DoF actuated joint, a 3-DoF spherical joint (S) and a 2-DoF universal joint (U) connecting the struts and the deformable platform. The mobility of the mechanism can be calculated by the Grübler criterion, when considering a general parallel mechanism with $n$ rigid links and $m$ joints, each joint having $f_i$-DoF and where $d$ stand for the mechanism motion system dimension, 6 in our case (spatial mechanism).

$$F = \lambda(n - j - 1) + \sum_{i=0}^{j} f_i = 6(11 - 14 - 1) + 28 = 4 \quad (1)$$

## III. Kinematic modeling

### A. Geometry of the manipulator

As shown in Fig. 3, the global coordinate system is located at the articulated spherical center of the central leg $\mathcal{F}_w = (O_w, X_w, Y_w, Z_w)$. $\mathcal{F}_p = (O_w, X_p, Y_p, Z_p)$ denote the frame attached to the configurable platform when $\theta = 0$.

For convenience, we define the following parameters for describing the geometry of the kinematic model. The struts have a total length $l_i$, where $i = 1, .., 4$ denotes the legs. The left part of the configurable platform is connected to the right part via a revolute joint and we

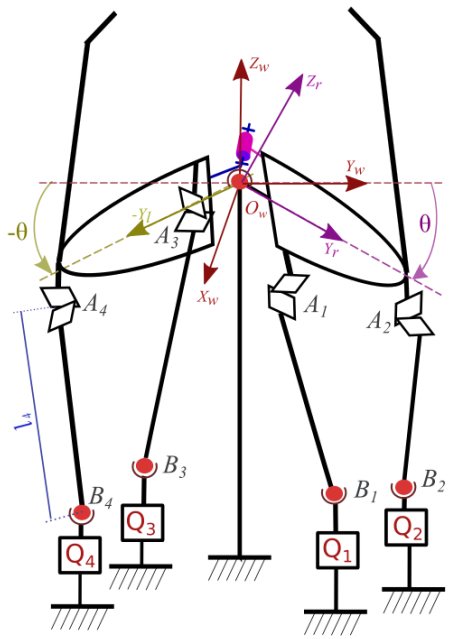


(a)

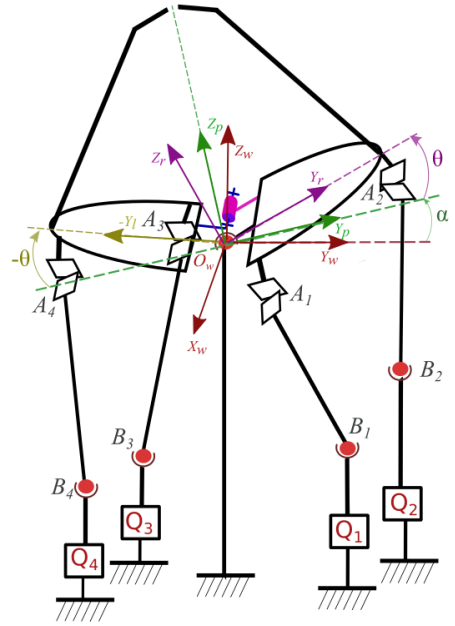


(b)

Fig. 3. The simplified kinematic model of the robot. (a) Pose where $\alpha = \beta = \gamma = 0$. (b) Pose where $\beta = \gamma = 0$.

define the relative rotation angle by $\theta$. The central strut is attached to the right part of the platform via a spherical joint $O_w$ and fixed at the base in the other end. The others struts are attached on one end to the platform through a universal joints ${}^wA_i$ and on the other to the mobiles bases on the other end via a spherical joint ${}^wB_i$.

The configurable platform carries the two fingers gripper. Each mobile base is attached to a linear vertical actuator.

$\mathcal{F}_r = (O_p, X_p, Y_r, Z_r)$ and $\mathcal{F}_l = (O_p, X_p, Y_l, Z_l)$ denote respectively the right and the left end-effector frame attached to the two parts of the platform. We define ${}^p\mathbf{R}_r$ and ${}^p\mathbf{R}_l$ 3-by-3 rotation matrix respectively between the moving frame $\mathcal{F}_r$ and the moving frame $\mathcal{F}_p$ and between the moving frame $\mathcal{F}_l$ and the moving frame $\mathcal{F}_p$.

$$\begin{cases} {}^p\mathbf{R}_r = rot(X_p, \theta), \\ {}^p\mathbf{R}_l = rot(X_p, -\theta), \end{cases} \tag{2}$$

Figure 3 presents the geometrical relationship between the 10 joints. We designate the coordinate of the 4 points at the top platform and the stage by ${}^wA_i$ and ${}^wB_i$ respectively. Figure 3 presents two poses of the wrist and the different frames related to the foldable platform.

### B. Positional constrain equations

The inverse kinematics aims to find the vertical displacement values of the four linear actuators, $q_i$ for $i = 1, .., 4$, for a given pose of the top platform. We denote the position of four points at the top foldable platform and the mobile bases by ${}^wA_i$ $(i = 1, .., 4)$ and ${}^wB_i$ $(i = 1, .., 4)$ respectively. The input variables are the rotation matrix ${}^w\mathbf{R}_p$ between the moving frame $\mathcal{F}_p$ and the reference frame $\mathcal{F}_w$ and the folding angle $\theta$ of the configurable platform. The position of the four universal joints ${}^wA_i$ on the top platform are given by:

$$\begin{cases} {}^wA_i = {}^w\mathbf{R}_p\, {}^p\mathbf{R}_r\, {}^rA_i, & i = 1, 2 \\ {}^wA_i = {}^w\mathbf{R}_p\, {}^p\mathbf{R}_l\, {}^lA_i, & i = 3, 4 \end{cases} \tag{3}$$

${}^wA_i$, ${}^rA_i$ and ${}^lA_i$ are the positions of $A_i$ expressed in $\mathcal{F}_w$, $\mathcal{F}_r$ and $\mathcal{F}_l$ respectively.

The position of the four spherical joints on the bottom of the struts ${}^wB_i$ are written as ${}^wB_i = [b_{xi} \quad b_{yi} \quad b_{zi} + q_i]^t$.

The constraint equations of the kinematic model are obtained by equating the distance between the joints on the base and joints on the platform to the strut length $l_i$, i.e the vector $A_iB_i$ norm :

$$\|{}^wB_i - {}^wA_i\| = l_i, \quad i = 1, .., 4 \tag{4}$$

$$(b_{xi}-a_{xi})^2+(b_{yi}-a_{yi})^2+(b_{zi}+q_i-a_{zi})^2 = l_i^2, \quad i = 1, .., 4 \tag{5}$$

To solve equation (5) we define the variables:

- $v_i = l_i^2 - (b_{xi} - a_{xi})^2 - (b_{yi} - a_{yi})^2$,
- $u_i = b_{zi} - a_{zi}$,

We can rewrite equation (5) as:

$$(u_i + q_i)^2 = v_i, \quad i = 1, .., 4 \tag{6}$$

Equation (6) gives two solutions for $q_i$, we must choose the one compatible with the actuator strokes.

### C. Velocity constraint equations

The instantaneous motion of the platform is obtained by taking the derivative of the kinematic equation 4 with respect to time and substituting with geometic parameters, written as:

$$\begin{cases} ({}^{w}B_i - {}^{w}A_i)^t([\Omega]_\times \, {}^{w}\mathbf{R}_p \, {}^{p}\mathbf{R}_r \, {}^{r}A_i + {}^{w}\mathbf{R}_p[{}^{p}X_p]_\times \, \omega_{(\theta)} \, {}^{p}\mathbf{R}_r \, {}^{r}A_i) \\ \qquad = ({}^{w}B_i - {}^{w}A_i)^t \dot{B}_i, \quad i = 1,2 \\ ({}^{w}B_i - {}^{w}A_i)^t([\Omega]_\times \, {}^{w}\mathbf{R}_p \, {}^{p}\mathbf{R}_l \, {}^{l}A_i - {}^{w}\mathbf{R}_p[{}^{p}X_p]_\times \, \omega_{(\theta)} \, {}^{p}\mathbf{R}_l \, {}^{l}A_i) \\ \qquad = ({}^{w}B_i - {}^{w}A_i)^t \dot{B}_i, \quad i = 3,4 \end{cases} \tag{7}$$

Here $\dot{B}_i = (0 \; 0 \; \dot{q}_i)^t$ is the instantaneous velocity of points ${}^{w}B_i$, where $\dot{q}_i$ represent the vertical speed of the four actuators on the base. In equation (7), $\Omega$ is the instantaneous angular velocity of the foldable platform where $\Omega = [\omega_{(\alpha)} \; \omega_{(\beta)} \; \omega_{(\gamma)}]^t$ and $\omega_{(\theta)}$ is the instantaneous angular velocity between the two parts of the platform. The symbol $[\Omega]_\times$ represents the cross product skew matrix.

We can write equation 7 in matrix form as:

$$J_l \, T = J_r \, \dot{Q} \tag{8}$$

where $T = [\omega_{(\alpha)} \; \omega_{(\beta)} \; \omega_{(\gamma)} \; \omega_{(\theta)}]^t$ is the motion twist of the configurable platform and $\dot{Q} = [\dot{q}_1, \; \dot{q}_2, \; \dot{q}_3, \; \dot{q}_4]^t$ is the actuating displacement of the linear motors. The left matrix $J_l$ has the following form:

$$\begin{bmatrix} ({}^{w}B_1 - {}^{w}A_1)^t(-[{}^{w}\mathbf{R}_p \, {}^{p}\mathbf{R}_r \, {}^{r}A_1]_\times \mid {}^{w}\mathbf{R}_p[{}^{p}X_p]_\times \, {}^{p}\mathbf{R}_r \, {}^{r}A_1) \\ ({}^{w}B_2 - {}^{w}A_2)^t(-[{}^{w}\mathbf{R}_p \, {}^{p}\mathbf{R}_r \, {}^{r}A_2]_\times \mid {}^{w}\mathbf{R}_p[{}^{p}X_p]_\times \, {}^{p}\mathbf{R}_r \, {}^{r}A_2) \\ ({}^{w}B_3 - {}^{w}A_3)^t(-[{}^{w}\mathbf{R}_p \, {}^{p}\mathbf{R}_l \, {}^{l}A_3]_\times \mid -{}^{w}\mathbf{R}_p[{}^{p}X_p]_\times \, {}^{p}\mathbf{R}_l \, {}^{l}A_3) \\ ({}^{w}B_4 - {}^{w}A_4)^t(-[{}^{w}\mathbf{R}_p \, {}^{p}\mathbf{R}_l \, {}^{l}A_4]_\times \mid -{}^{w}\mathbf{R}_p[{}^{p}X_p]_\times \, {}^{p}\mathbf{R}_l \, {}^{l}A_4) \end{bmatrix} \tag{9}$$

The right matrix $J_r$ has the following form:

$$J_r = \begin{bmatrix} a_{z1} - b_{z1} & \cdots & 0 \\ \vdots & \ddots & \vdots \\ 0 & \cdots & a_{z4} - b_{z4} \end{bmatrix} \tag{10}$$

The inverse of the Jacobian matrix relating the four actuator inputs $\dot{Q}$ to the motion twist T is

$$\dot{Q} = J^{-1} \, T = J_r^{-1} J_l \, T \tag{11}$$

## IV. Design and analysis of the mechanism

This part describes the geometry and the design of the wrist to present good properties of motion. Then a model at scale 4:1 is realized and actuated as a proof-of-concept.

### A. Mechanical design of the robot

Thanks to the symmetrical proprieties of the architecture, the kinematic design parameters can be reduced to a relatively few numbers. Assuming identical lengths for the 4 moving struts $l_i$, identical distance between the joints fixed on the platform ${}^{w}A_i$, the joints ${}^{w}B_i$ are symmetrically fixed to the mobile actuated bars. The spherical joint connected to the base and the revolute joint are disposed at the same axis $(O_w, X_p)$, see Fig. 4. Two configurations of the moving struts are possible, either crossed or parallel.

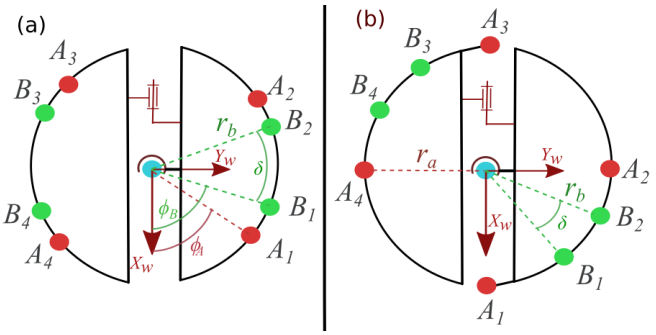


Fig. 4. Geometrical description of the top foldable platform and the bottom joints. (a) Presentation of all parameters. (b) Particular case where $\phi_A = 0$

The objective of this part is the validation of the proposed structure using 3D printing model. Fig. 5 depicts a CAD view of the prototype designed in SolidWorks. The actuators take place away from the structure, where there is no spacial constraints to the size and the position, which gives us a wider range of motion of the foldable wrist.

The selected kinematic design parameters are : $l_i = 34mm$, $r_a = r_b = 16mm$, $\delta = 40°$ and $\phi_A = 0$.

These parameters were therefore constrained by the technical fabrication of the prototype using a 3D printer, these the size of the model is 4 times bigger than the intended size.

### B. Workspace analysis

The workspace of the mechanism refers to the set of all positions and orientations achievable by the end-effector frame. We analyzed the theoretical workspace of the manipulator in order to assess the capabilities and the limitation of the system. The theoretical workspace is obtained by assuming a travel motion of 20mm of the actuators. The red and the blue ranges shows the two reachable space of the two fingers of the gripper. The tridimensional workspace of the two distal fingers of the end-effector of the 4-DoF is shown in Fig. 6. The illustrated surface is determined by the combination of two partial surfaces that presents the individual maximum working ranges of each finger. This includes the surface, which is the superposition of the two fingers where the manipulator can be used as a scissors. Table I shows the maximum rotation angles in degrees of the wrist using the chosen kinematic design parameters and a 20mm travel motion of the actuators.

### C. Experimental results

For the proof-of-concept, a functioning experimental prototype has been constructed using a 3D printing machine in Acrylic plastic. It consists of four vertical moving struts and a fixed central struts, each of the

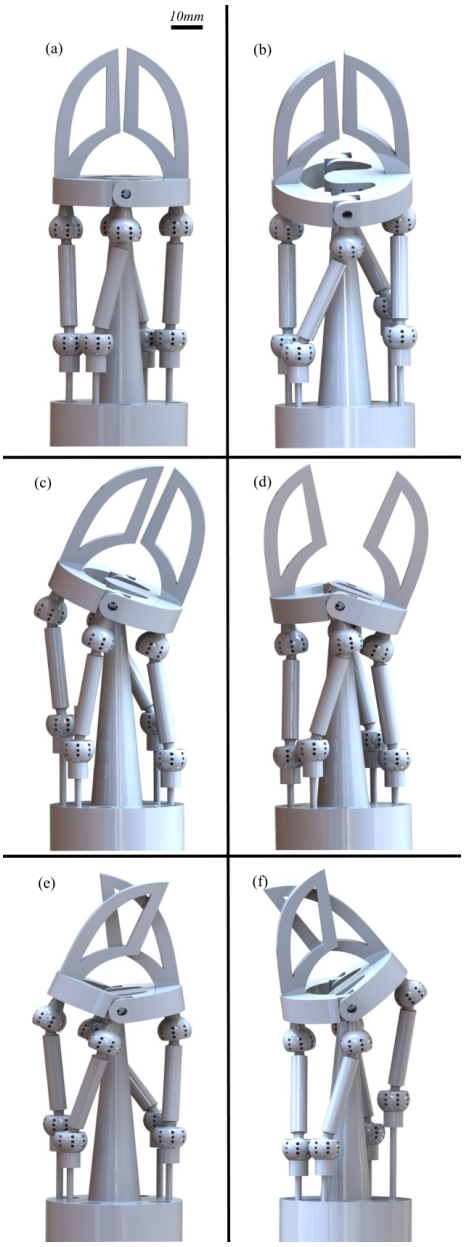


Fig. 5. Schematic drawing of the manipulator. (a) Manipulator at the home position. (b) Angular rotation about the y-axis. (c) Angular rotation about the x-axis.(d) Gripper opening. (e) Gripper closing. (f) Gripper closing and angular rotation about the y-axis.

TABLE I

THE MAXIMUM ROTATION ANGLES OF THE WRIST USING 20MM TRAVEL MOTION OF THE ACTUATORS

| | max | min |
|---|---|---|
| $\alpha$ (deg) | 52 | -52 |
| $\beta$ (deg) | 40 | -40 |
| $\gamma$ (deg) | 66 | -66 |
| $\theta$ (deg) | 33 | -60 |

moving struts is attached through two spherical joints at their end to the foldable platform and the moving rods (we have chosen to use spherical joints instead of universal ones because of the easiness of fabrication). The

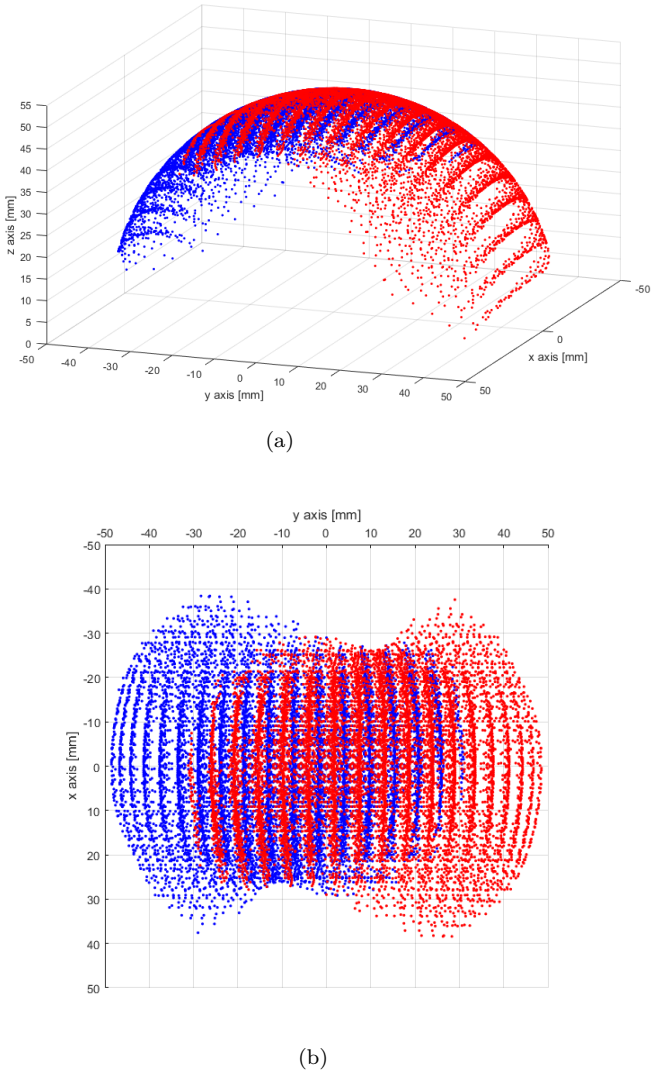


Fig. 6. Workspace of the two fingers of the wrist. (a) spacial presentation of the workspace. (b) Top view of the workspace.

movement of each rods is insured by a 1-DoF servo-motor located away from the structure.

The whole prototype was printed in one block including the spherical joints. The clearance fits used in spherical joints was chosen to comply the technical resolution limit of the 3D printing machine, to a minimum value of 0.1mm. The left part of the foldable platform is attached to the right one via two revolute joints. Each finger of the gripper/scissors are a part of the platform.

The main interest of fabrication of this robot is to validate the mechanism structure. The purpose of our experiment is to show that, when the rods translate, the robot structure deforms and the top platform reaches the desired orientation and angular deflection. The end-effectors are non-standard part of the wrist. Their geometry can be adapted to the task to operate.

Figure 7 shows the wrist controlled with a joystick. The proposed motion control algorithm was successfully


Fig. 7. Manipulation of the wrist through a joystick.

implemented on the prototype to carry out the control motion of the joystick with the 4-DoFs in rotations. They can be further appreciated in the video clip accompanying this paper.

## V. conclusion and outlook

In this paper, we proposed a new concept of a robotic structure designed for minimally invasive surgery. This wrist is able to grasp/cut objects (1-DoF) and achieve rotations with 3-DoF by actuating four linear external actuators. Initially, the kinematic structure of the robot has been investigated. Then, the inverse kinematic has been determined and a workspace analysis have been likewise performed to evaluate the theoretical capabilities and effectiveness of the system. A first wrist prototype of the design described in the paper has been fabricated at a larger scale and tested. Future works will address a reduction in robot size and the optimization of the design of the structure and the shape of the gripper/scissors. In addition, the characterization of the manipulator singularities in the control and further analysis regarding the operation with the wrist will be performed.

## Acknowledgments

This work has been supported by Région de Bourgogne-Franche-Comté, Labex ACTION project (ANR-11-LABX-01-01) and Equipex ROBOTEX project (ANR-10-EQPX-44-01). Authors acknowledge the French RENATECH network and its FEMTO-ST technological facilities MIMENTO.

## References

[1] R. J. Leveillee, S. M. Castle, M. A. Gorin, N. Salas, and V. Gorbatiy, "Initial experience with laparoendoscopic single-site simple nephrectomy using the transenterix spider surgical system: assessing feasibility and safety," *Journal of Endourology*, vol. 25, no. 6, pp. 923–925, 2011.

[2] S. Lescano, M. Rakotondrabe, and N. Andreff, "Precision prediction using interval exponential mapping of a parallel kinematic smart composite microstructure," in *IEEE/RSJ International Conference on Intelligent Robots and Systems (IROS)*, 2015, pp. 1994–1999.

[3] V. Vitiello, S.-L. Lee, T. P. Cundy, and G.-Z. Yang, "Emerging robotic platforms for minimally invasive surgery," *IEEE Reviews in Biomedical Engineering*, vol. 6, pp. 111–126, 2013.

[4] P. Noel, M. Nedelcu, and M. Gagner, "Spider® sleeve gastrectomy–a new concept in single-trocar bariatric surgery: Initial experience and technical details," *Journal of visceral surgery*, vol. 151, no. 2, pp. 91–96, 2014.

[5] S. Can, C. Staub, A. Knoll, A. Fiolka, A. Schneider, and H. Feussner, "Design, development and evaluation of a highly versatile robot platform for minimally invasive single-port surgery," in *4th IEEE RAS & EMBS International Conference on Biomedical Robotics and Biomechatronics (BioRob)*, 2012, pp. 817–822.

[6] S. Lescano, M. Rakotondrabe, and N. Andreff, "Micromechanisms for laser phonosurgery: A review of actuators and compliants parts." in *IEEE International Conference on Biomedical Robotics and Biomechatronics, BIOROB'12.*, 2012, pp. 3–pages.

[7] D. J. Abbott, C. Becke, R. I. Rothstein, and W. J. Peine, "Design of an endoluminal notes robotic system," in *IEEE/RSJ International Conference on Intelligent Robots and Systems (IROS)*, 2007, pp. 410–416.

[8] T. Do, T. Tjahjowidodo, M. Lau, and S. Phee, "Adaptive control for enhancing tracking performances of flexible tendon–sheath mechanism in natural orifice transluminal endoscopic surgery (notes)," *Mechatronics*, vol. 28, pp. 67–78, 2015.

[9] J. H. Kaouk, R. K. Goel, G.-P. Haber, S. Crouzet, and R. J. Stein, "Robotic single-port transumbilical surgery in humans: initial report," *BJU international*, vol. 103, no. 3, pp. 366–369, 2009.

[10] A. D. Pryor, J. R. Tushar, and L. R. DiBernardo, "Single-port cholecystectomy with the transenterix spider: simple and safe," *Surgical endoscopy*, vol. 24, no. 4, pp. 917–923, 2010.

[11] M. Niccolini, G. Petroni, A. Menciassi, and P. Dario, "Real-time control architecture of a novel single-port laparoscopy bimanual robot (sprint)," in *IEEE International Conference on Robotics and Automation (ICRA)*, 2012, pp. 3395–3400.

[12] J.-P. Merlet, *Parallel robots*. Springer Science & Business Media, 2006, vol. 128.

[13] ——, "Optimal design for the micro parallel robot mips," in *IEEE International Conference on Robotics and Automation (ICRA'02)*, vol. 2, 2002, pp. 1149–1154.

[14] V. Nabat, R. de la O, O. María, O. Company, S. Krut, and F. Pierrot, "Par4: very high speed parallel robot for pick-and-place," in *IEEE/RSJ International Conference on Intelligent Robots and Systems (IROS)*, 2005, pp. 553–558.

[15] B.-J. Yi, H. Y. Na, J. H. Lee, Y.-S. Hong, S.-R. Oh, I. H. Suh, and W. K. Kim, "Design of a parallel-type gripper mechanism," *The International Journal of Robotics Research*, vol. 21, no. 7, pp. 661–676, 2002.

[16] M. G. Mohamed and C. M. Gosselin, "Design and analysis of kinematically redundant parallel manipulators with configurable platforms," *IEEE Transactions on Robotics*, vol. 21, no. 3, pp. 277–287, 2005.

[17] P. Lambert and J. L. Herder, "Self dual topology of parallel mechanisms with configurable platforms," in *Computational Kinematics*. Springer, 2014, pp. 291–298.

[18] P. Lambert and J. Herder, "A novel parallel haptic device with 7 degrees of freedom," in *World Haptics Conference (WHC)*, 2015, pp. 183–188.